Rationale and mechanism for the low photoinactivation rate of bacteria in plasma

Jie Chen[a,b], Thomas C. Cesario[c], and Peter M. Rentzepis[b,1]

[a]Key Laboratory for Laser Plasmas (Ministry of Education) and Department of Physics and Astronomy, Shanghai Jiao Tong University, Shanghai 200240, China; [b]Department of Chemistry, University of California, Irvine, CA 92697; and [c]School of Medicine, University of California, Irvine, CA 92697

The rate of bacterial photoinactivation in plasma by methylene blue (MB), especially for Gram-negative bacteria, has been reported to be lower, by about an order of magnitude, than the rate of inactivation in PBS and water solutions. This low inactivation rate we attribute to the bleaching of the 660-nm absorption band of MB in plasma that results in low yields of MB triplet states and consequently low singlet oxygen generation. We have recorded the change of the MB 660-nm-band optical density in plasma, albumin, and cysteine solutions, as a function of time, after 661-nm excitation. The transient triplet spectra were recorded and the singlet oxygen generated in these solutions was determined by the rate of decrease in the intensity of the 399-nm absorption band of 9, 10-anthracene dipropionic acid. We attribute the bleaching of MB, low singlet oxygen yield, and consequently the low inactivation rate of bacteria in plasma to the attachment of a hydrogen atom, from the S–H group of cysteine, to the central nitrogen atom of MB and formation of cysteine dimer.

ADPA | photoinactivation deficiency | Leuco methylene blue | electrophilic attack | transient spectroscopy

Even though infections from bacterially contaminated plasma are thought to be very few (1) and the frequency of patient sepsis caused by transfusion of blood contaminated by bacteria is as low or less than the transfusion-associated hepatitis C virus infection (2), the possibility of such infection cannot be entirely discounted in view of the fact that new or even more resistant strains of known bacteria are being encountered. To a large extent, pooled human plasma is sterilized by the solvent–detergent method (3–5), whereas single-donor human plasma is often decontaminated by methylene blue (MB) photoexcitation, which generates reactive oxygen species that safely inactivate many viruses (6, 7). However, several Gram-positive and especially Gram-negative bacteria are found to be very resistant to photoinactivating agents such as porphyrins and thiazine dyes, possibly because the outer walls of Gram-negative bacteria, such as *Serratia marcescens* (SM), are composed of negatively charged lipopolysaccharides, which are resistant to photoinactivation by these dyes (8).

Gram-positive bacteria and several Gram-negative bacteria are relatively easily inactivated, especially in high-pH MB–PBS solutions, after irradiation with 661-nm light for a rather short period, i.e., 10 min (9). Gram-negative bacteria usually require longer exposure times for inactivation. Table 1 lists the time required for the inactivation of two representative bacteria, coagulase-negative *Staphilocci*, CoNS (Gram-positive) and SM (Gram-negative). Inactivation of bacteria dispersed in PBS at pHs 7 and 9 occurs within 20 min or less; however, note that when the same concentration of bacteria, 10^7/mL, was dispersed in a solution of human plasma containing 2×10^{-5} M MB and irradiated with the same photon flux of 6.8-mW, 661-nm light-emitting diode (LED) light, the inactivation rate was found to be an order of magnitude lower than that of the same bacteria in PBS and saline water solutions (10). This inactivation deficiency, observed in plasma, cannot be attributed to the decrease in light intensity due to absorption or scattering, because the fresh human plasma used is clear and neither absorbs in the 661-nm excitation wavelength region nor scatters the LED light. Singlet oxygen is the dominant active species responsible for the photoinactivation of bacteria (11–21), with MB being the primary photosensitizing agent used for the generation of singlet oxygen and the sterilization of plasma (22–27). To that effect we investigated possible reactions between plasma and MB that may be responsible for decrease in singlet oxygen generation that would explain the low bacteria inactivation rate in plasma.

The data presented show that the 660-nm absorption band of MB is bleached when MB solutions in plasma, albumin, or cysteine are excited with 661-nm LED light, but not those of MB γ-globulin or fibrinogen solutions (Fig. 1). The amount of singlet oxygen generated in MB–plasma, MB–albumin, and MB–cysteine solutions is found to be drastically less than that in MB–PBS solutions. A mechanism for the bleaching of MB in plasma is proposed based on the attachment of H atoms, from the S–H group of cysteine to the central nitrogen atom of MB, that destroys the MB ring conjugation (Scheme 1), thus initiating bleaching of the 660-nm MB absorption band, where RSH is cysteine and RSSR is the cysteine dimer, cystine.

Results and Discussion

When MB dissolved in aqueous or PBS solutions is excited into its first excited singlet state (Fig. 2), it decays with nanoseconds lifetime to the first excited triplet state, $^3MB^*$, reaction **1** (28). The absorption band of the triplet state, $^3MB^*$, located in the $11,400\text{-cm}^{-1}$ region (10, 28, 29), (Fig. 2) has been determined by means of picosecond spectroscopy and computer calculations to decay in oxygen-free and oxygenated solutions, with rates of 2.7×10^9 s^{-1} and 1×10^9 s^{-1}, respectively (28, 30, 31). The triplet state, in turn, may transfer its energy to ground-state triplet oxygen, $^3O_2$, promoting the formation of excited singlet oxygen, $^1O_2$ ($^1\Delta_g$), reaction **2** (21, 29). The $^1O_2$ singlet oxygen lifetime is reported to be 3 and 53 μs in H_2O and D_2O, respectively (32). Because of its high reactivity, about 100-Å free mean reaction path (33, 34), singlet oxygen reactions with bacteria are most efficient when the singlet oxygen photogenerating molecule is in contact

Significance

Human plasma is often decontaminated by methylene blue (MB) photoexcitation; however, the rate of bacterial photo-inactivation in plasma has been found to be lower by about an order of magnitude than that in PBS or water. We attribute this low inactivation rate to the bleaching of the 660-nm band of MB by the electrophilic attack of the S–H group of cysteine on the central nitrogen atom. Further investigations are aimed at the development of means that prevent bleaching of MB and allow its photoinactivation of bacteria and other pathogens.

Table 1. Inactivation of Gram-positive and Gram-negative bacteria in MB–PBS and MB–plasma solutions as a function of irradiation time with 6.8-mW, 661-nm LED light

Bacteria type/solution	Gram $^{+/-}$	Inactivation time, min		
		pH5	pH7	pH9
ATCC 12228 coagulase-negative *Staphilcocci epidermidis*–PBS	+	5	1	0.5
ATCC 12228 coagulase-negative *S. epidermidis*–plasma	+	30	30	30
ATCC 13477 *Serratia marcescens*–PBS	−	60	10	10
ATCC 13477 *S. marcescens*–plasma	−	>120	>120	>120

or very close to the bacteria wall. The formation of singlet oxygen is shown in this paper to be diminished when MB in plasma solution was excited with 661-nm LED light.

$$MB + h\nu \rightarrow {}^1MB^* \rightarrow {}^3MB^*, \qquad [1]$$

$$^3MB^* + {}^3O_2 \rightarrow MB + {}^1O_2({}^1\Delta_g), \quad k_2 = 2.4 \times 10^9 M^{-1} \cdot s^{-1}. \qquad [2]$$
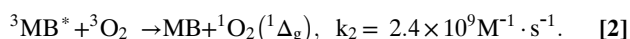
Solutions of 2×10^{-5} M MB in plasma and PBS were illuminated with 661-nm LED light and the change in the optical density (OD) of the 663-nm MB absorption band was recorded as a function of irradiation time and is displayed in Fig. 1. Fig. 1 also shows similar experimental data for the decrease of the 663-nm-band OD vs. time for MB–albumin and MB–cysteine solutions. Comparison of the MB 663-nm absorption band bleaching in these four MB solutions shows that in MB–PBS solution the 663-nm OD hardly changes, whereas in the other three solutions MB bleaches within a few minutes. These data suggest that a plasma component, quite possibly cysteine, interacts with the excited MB to form a leuco-type MB (LMB) molecule. It was also found that the 288-nm MB absorption band decreases during the bleaching of MB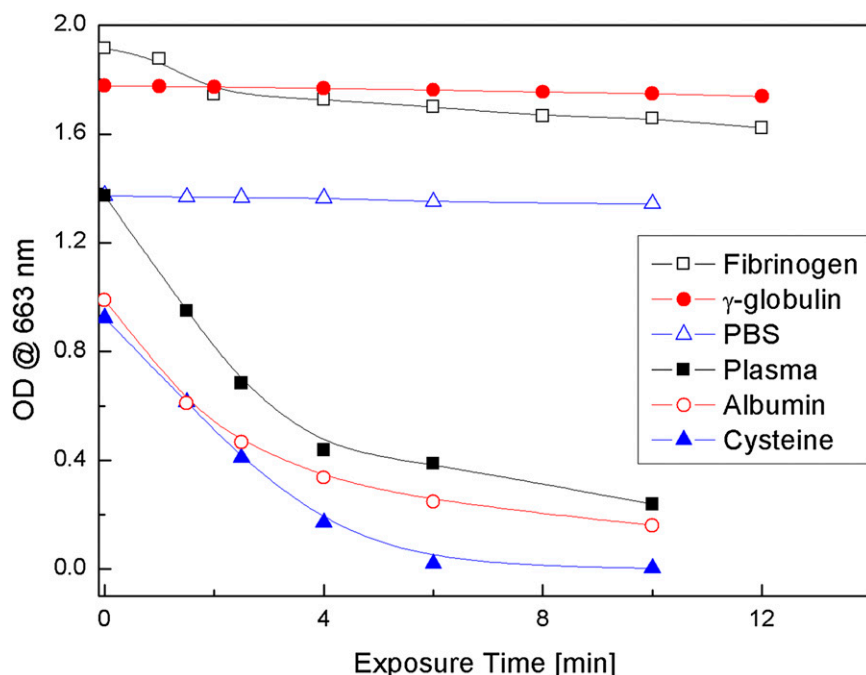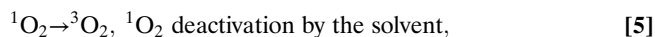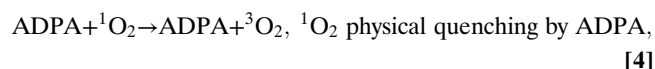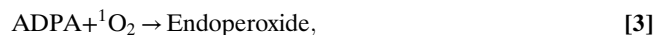 in cysteine solutions, whereas the ~250-nm absorption band of cystine is formed (Fig. 3). The net result is a decrease in the 664- and 288-nm MB absorption OD and an increase in the 250-nm cystine absorption OD (Fig. 4). The increase in the 250-nm absorption band OD is attributed to cystine, the dimeric form of cysteine,

which is formed by the oxidation reaction of cysteine with MB (Scheme 1). Ultrafast time-resolved MB triplet-state spectra showed that bleaching of MB inhibits the formation of MB triplets, in agreement with previous reports (10, 28). These studies also showed that the intensity of the ~845-nm MB transient triplet-state spectra in plasma, albumin, and cysteine decreased by more than a factor of 2 compared with those in PBS and water solutions, (Fig. 2) during 661-nm irradiation.

The decrease in MB triplet formation implies that the amount of singlet oxygen generated should also be lower in the plasma, albumin, and cysteine solutions than in water or PBS. The change of 9,10-anthracene dipropionic acid(ADPA) 378- and 399-nm absorption bands (Fig. 5) is due to the reaction of ADPA with singlet oxygen, ${}^1O_2$ $({}^1\Delta_g)$, to form endoperoxide, ADPA-O_2 (32), Scheme 2. Because the endoperoxide does not absorb in the 350–450-nm region, where ADPA exhibits three absorption bands, the decrease in the ADPA 399-nm absorption band OD is a direct measure of amount of singlet oxygen generated in the solution, reaction **3** (35):

$$ADPA + {}^1O_2 \rightarrow Endoperoxide, \qquad [3]$$

$$ADPA + {}^1O_2 \rightarrow ADPA + {}^3O_2, \; {}^1O_2 \text{ physical quenching by ADPA}, \qquad [4]$$

$$^1O_2 \rightarrow {}^3O_2, \; {}^1O_2 \text{ deactivation by the solvent}, \qquad [5]$$

Fig. 1. OD decrease of the 663-nm absorption band of MB in fibrinogen, γ−globulin, PBS, plasma, albumin, and cysteine solution as a function of 661-nm LED exposure time.

Fig. 2. Absorption spectra of 2×10^{-5} M MB in PBS (black solid curve with left axis) and transient absorption spectra of the singlet excited state (red dashed curve with right axis) and the triplet excited state (blue dotted curve with right axis) of 6.4×10^{-5} M MB solution.

$$k_3 + k_4 = 8.2 \times 10^7 M^{-1} \cdot s^{-1}, \quad k_5 = 2.5 \times 10^5 \ s^{-1} \ (ref. 35).$$

Cysteine, albumin, plasma, and ADPA do not absorb in the 660-nm spectral region where MB is excited; therefore, solutions of these molecules with MB and ADPA would be expected to generate equal amounts of singlet oxygen, unless they react with MB or ADPA in a manner that inhibits the formation of singlet oxygen. Spectroscopic measurements confirm that the ADPA spectrum is not altered or decreased after the addition of albumin, cysteine, or plasma to the MB–ADPA–PBS solution and no reaction was found to take place in the absence of irradiation.

In oxygen-free solutions, i.e., nitrogen-saturated MB–ADPA solutions, endoperoxide was not formed but the intensity of the 399-nm ADPA absorption band decreased by <10%, after 661-nm irradiation, owing to the reaction of ADPA with the MB excited triplet state. However, energy transfer from the MB triplet state to the ADPA triplet state is not favored because the 11,500-cm^{-1} MB triplet state lies below the ADPA triplet-state band located at 14,500 cm^{-1} (32). Therefore, to a very large extent, the slope of the ADPA 399-nm OD decay versus irradiation time is proportional to the amount of singlet oxygen generated, and the ratio of the

slopes, measured in the four solutions, provides a measure of the relative yield of singlet oxygen in each of these solutions (35, 36).

Solutions of 2×10^{-5} M MB–ADPA solution in plasma and PBS were irradiated with 661-nm monochromatic LED light and the decay of the 399-nm ADPA absorption band was recorded as a function of irradiation time (Fig. 6). The slopes of the ADPA absorption band decay curves in MB–PBS and MB–plasma solutions were calculated to be $1.1 \times 10^{-2} \cdot s^{-1}$ and $1.1 \times 10^{-3} \cdot s^{-1}$, respectively, and the ratio of the PBS to plasma slopes was 10, which implies that the amount of singlet oxygen generated under identical conditions in plasma is an order of magnitude less than the amount of singlet oxygen generated in PBS or water solutions.

We proceeded further to determine which plasma component is responsible for the observed low singlet oxygen production in plasma. To that effect, we performed similar experiments using solutions of MB–ADPA with the addition of 3×10^{-5} M of each of the three major plasma proteins: fibrinogen, γ-globulin, and human serum albumin. Fibrinogen and γ-globulin displayed practically the same 399-nm OD ADPA decay kinetics, after illumination with the 661-nm LED, as the MB–ADPA–PBS solution. However, when human serum albumin–MB–ADPA–PBS solution was irradiated with the same 661-nm LED beam, the

Fig. 3. Time-resolved spectra of the 288- and 664-nm MB absorbance decreases and ~250-nm cystine absorbance increases from 0 to 2 min after cysteine–MB aqueous solution irradiated with 661-nm light.
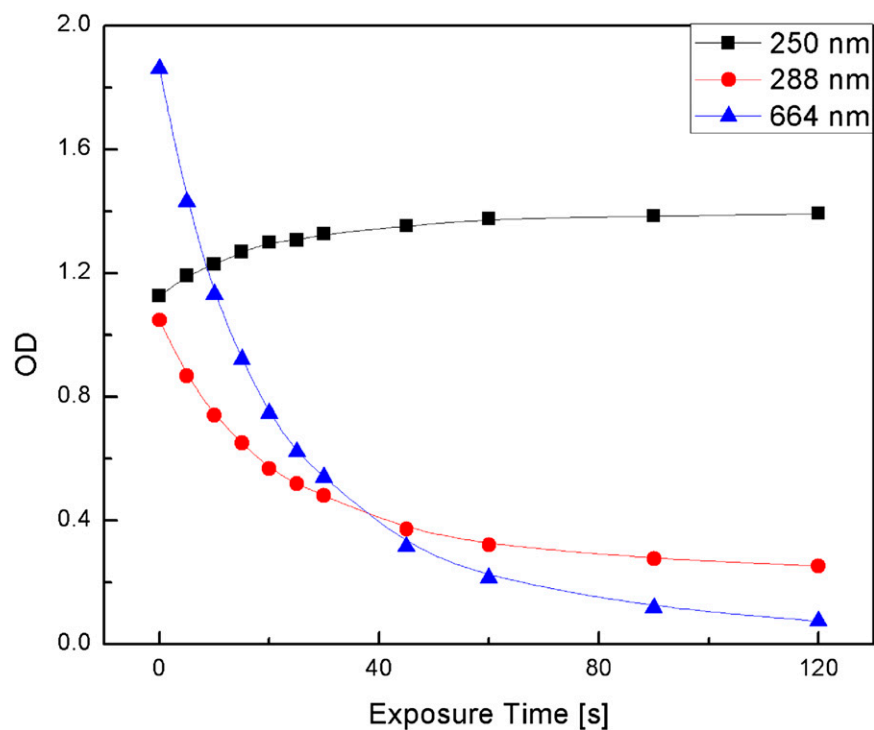
Fig. 4. OD changes of the 288- and 664-nm MB bands and 250-nm cystine band as a function of irradiation time, after cysteine–MB aqueous solution irradiated with 661-nm light.

399-nm ADPA absorption band was found to decay with a rate of $1.2 \times 10^{-4} \cdot s^{-1}$, which is much slower than the rate measured for PBS and even plasma solutions (Fig. 6). The ratio of the slopes of PBS to albumin solutions was found to be 92, indicating that the amount of singlet oxygen generated in albumin–MB solutions is about 100× smaller than in PBS–MB solutions.

Albumin is a large protein molecule composed of several distinct components, including cysteine amino acid. Because cysteine contains a S–H group which may react with MB, we studied the effect of cysteine on both the bleaching of MB, discussed and depicted in Fig.1, and also on its influence in the generation of singlet oxygen by MB excited with the 661-nm LED light. To that effect, 1×10^{-5} M cysteine added to the MB–ADPA–PBS solution was irradiated with the same photon flux of 661-nm LED beam as the other solutions. The decay of the 399-nm ADPA band OD, shown in Fig. 6, is calculated to be $6.7 \times 10^{-4} \cdot s^{-1}$ and the ratio of the PBS to cysteine slopes is found to be 14. These data suggest that MB–PBS solutions generate more than one order of magnitude more singlet oxygen than MB–cysteine
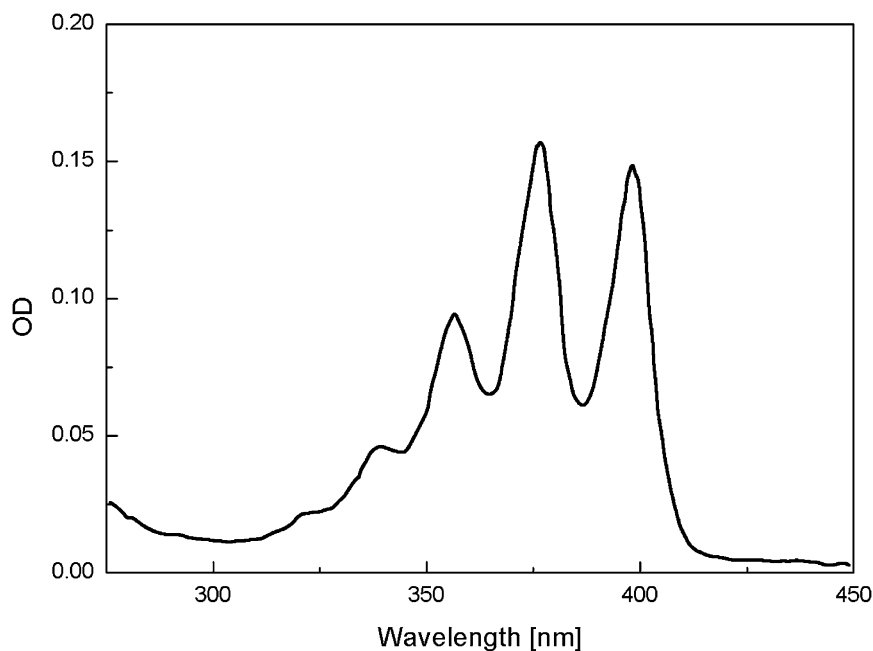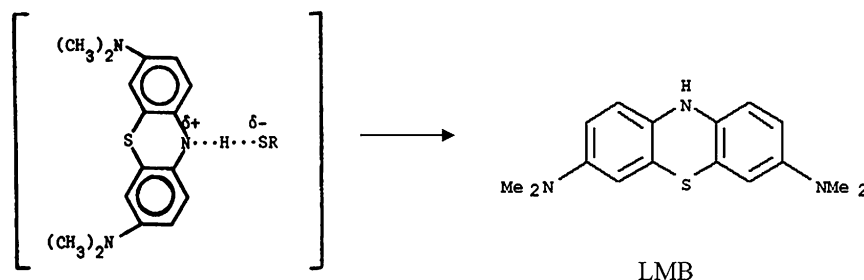

Fig. 5. Absorption spectra of ADPA in PBS.

Fig. 6. Decrease of the 399-nm absorption band of ADPA–MB in PBS, plasma, albumin, and cysteine solution as a function of 661-nm LED exposure time.

solutions under the similar experimental conditions. Because the concentrations of MB and ADPA are the same in all solutions and the irradiating photon fluxes are equal, we attribute the differences in the ADPA 399-nm decay slope to the reaction of cysteine with MB.

We propose that excited MB reacts with cysteine, causing the abstraction of the electrophilic H atom of the S–H group and its

of the 660-nm MB absorption band and formation of a leuco-type MB. The bleaching inhibits formation of MB triplet states and singlet oxygen in these solutions and consequently is the reason for the observed much lower inactivation rates of bacteria in plasma compared with that in PBS solutions. Electron abstraction that involves the MB radical, which is an electron donor, and the thiol,

Scheme 1.

attachment onto the central nitrogen atom of the excited MB molecule, thus destroying the conjugation of the MB ring structure (Scheme 3) and resulting in the observed strong bleaching

which is a rather strong electron acceptor, is also possible. In addition, electron transfer from the RS^- group to form MB^-, the conjugate base of the acidic leuco-MB, cannot be discounted.

Assuming that the bacteria inactivation process proceeds via oxidation of the bacteria wall by singlet oxygen that leads to the destruction of DNA, the data presented provide a plausible mechanism and explanation for the observed very low rate of bacteria photoinactivation in plasma. The data presented also show that the amount of singlet oxygen formed in plasma is an order of magnitude lower than the amount generated in water or PBS solutions, which is in agreement with previously published data on MB triplet-state formation in plasma (10). In addition, we show that the attachment of the H atom from the S–H group of cysteine is quite possibly responsible for the MB bleaching and the low rate of bacteria inactivation in plasma. It will be, therefore, interesting and rather important for the efficient photoinduced inactivation of pathogens in plasma to use a molecule

Scheme 2.

LMB

Scheme 3.

that binds onto the cysteine component of the human plasma, thus preventing the electrophilic attack of the S–H group of cysteine on the central nitrogen atom of MB, and henceforth allows MB to generate the same amount of singlet oxygen in plasma as is generated in water or PBS solutions. We are investigating such chemicals and photochemical processes, restricted to molecules that do not denature human plasma.

Materials and Methods

Plasma was obtained from the blood bank as commercially available pooled human plasma, no longer useful for human administration. It was kept refrigerated and the procedure was performed with the approval of the Institutional Review Board. MB, albumin, and cysteine were purchased from Sigma-Aldrich and used without further purification. As shown in Fig. 2, 2×10^{-5} M MB dissolved in water or PBS consists mostly of monomers evidenced by the absence of the short wavelength shoulder, ~612 nm, in the 660-nm absorption band. Plasma or PBS were mixed with 2×10^{-5} M MB–distilled

water solution and their absorption spectra were recorded with a Shimatsu 1600 UV spectrophotometer, using 1-cm optical path-length quartz cells, unless stated otherwise. Two-mL samples were placed in open quartz cuvettes and irradiated for a preselected period with 6.8-mW, 661-nm monochromatic LED light. The solutions were kept at ~4 °C and irradiated in cuvettes placed on ice. The absorption spectra of the irradiated samples were also recorded and the 663-nm OD decrease was calculated and plotted in Fig. 1.

Subsequently, 1 mL of 1×10^{-4} M ADPA was added to each solution and the relative amount of singlet oxygen generated in each solution was determined by recording the decrease in the 399-nm absorption band OD of ADPA as a function of 661-nm irradiation time as shown in Fig. 6. The slope of the 399-nm OD decay curve is a measure of the amount of singlet oxygen generated and the ratio of the slopes between two solutions is a measure of the relative amount of singlet oxygen generated in each solution (32).

1. Wagner SJ, Friedman LI, Dodd RY (1994) Transfusion-associated bacterial sepsis. *Clin Microbiol Rev* 7(3):290–302.
2. Kleinman S, et al. (1992) Increased detection of hepatitis C virus (HCV)-infected blood donors by a multiple-antigen HCV enzyme immunoassay. *Transfusion* 32(9):805–813.
3. Prince AM, Horowitz B, Brotman B (1986) Sterilisation of hepatitis and HTLV-III viruses by exposure to tri(n-butyl)phosphate and sodium cholate. *Lancet* 1(8483):706–710.
4. Dichtelmüller HO, et al. (2009) Robustness of solvent/detergent treatment of plasma derivatives: A data collection from Plasma Protein Therapeutics Association member companies. *Transfusion* 49(9):1931–1943.
5. Hellstern P, Solheim BG (2011) The use of solvent/detergent treatment in pathogen reduction of plasma. *Transfus Med Hemother* 38(1):65–70.
6. Pelletier JPR, Transue S, Snyder EL (2006) Pathogen inactivation techniques. *Best Pract Res Clin Haematol* 19(1):205–242.
7. Mohr H, Lambrecht B, Selz A (1995) Photodynamic virus inactivation of blood components. *Immunol Invest* 24(1-2):73–85.
8. Nikaido H (1989) Outer membrane barrier as a mechanism of antimicrobial resistance. *Antimicrob Agents Chemother* 33(11):1831–1836.
9. Chen J, Cesario TC, Rentzepis PM (2011) Effect of pH on methylene blue transient states and kinetics and bacteria photoinactivation. *J Phys Chem A* 115(13):2702–2707.
10. Er AO, Chen J, Cesario TC, Rentzepis PM (2012) Inactivation of bacteria in plasma. *Photochem Photobiol Sci* 11(11):1700–1704.
11. Wainwright M, Phoenix DA, Rice L, Burrow SM, Waring J (1997) Increased cytotoxicity and phototoxicity in the methylene blue series via chromophore methylation. *J Photochem Photobiol B* 40(3):233–239.
12. Lambrecht B, Mohr H, Knüver-Hopf J, Schmitt H (1991) Photoinactivation of viruses in human fresh plasma by phenothiazine dyes in combination with visible light. *Vox Sang* 60(4):207–213.
13. Ruane PH, et al. (2004) Photochemical inactivation of selected viruses and bacteria in platelet concentrates using riboflavin and light. *Transfusion* 44(6):877–885.
14. Demidova TN, Hamblin MR (2004) Photodynamic therapy targeted to pathogens. *Int J Immunopathol Pharmacol* 17(3):245–254.
15. Tardivo JP, et al. (2005) Methylene blue in photodynamic therapy: From basic mechanisms to clinical applications. *Photodiagn Photodyn Ther* 2(3):175–191.
16. Nakimbugwe D, Masschalck B, Anim G, Michiels CW (2006) Inactivation of gram-negative bacteria in milk and banana juice by hen egg white and lambda lysozyme under high hydrostatic pressure. *Int J Food Microbiol* 112(1):19–25.
17. Carvalho CMB, et al. (2007) Photoinactivation of bacteria in wastewater by porphyrins: Bacterial beta-galactosidase activity and leucine-uptake as methods to monitor the process. *J Photochem Photobiol B* 88(2-3):112–118.
18. Schastak S, Gitter B, Handzel R, Hermann R, Wiedemann P (2008) Improved photoinactivation of gram-negative and gram-positive methicillin-resistant bacterial strains using a new near-infrared absorbing meso-tetrahydroporphyrin: a comparative study with a chlorine e6 photosensitizer photolon. *Methods Find Exp Clin Pharmacol* 30(2):129–133.
19. Gollnick K (1968) *Type II Photooxygenation Reactions in Solution. Advances in Photochemistry* (Wiley, New York), pp 1–122.
20. Foote CS (1968) Mechanisms of photosensitized oxidation. There are several different types of photosensitized oxidation which may be important in biological systems. *Science* 162(3857):963–970.
21. Fisher AMR, Murphree AL, Gomer CJ (1995) Clinical and preclinical photodynamic therapy. *Lasers Surg Med* 17(1):2–31.
22. Skripchenko AA, Wagner SJ (2000) Inactivation of WBCs in RBC suspensions by photoactive phenothiazine dyes: Comparison of dimethylmethylene blue and MB. *Transfusion* 40(8):968–975.
23. Williamson LM, Cardigan R, Prowse CV (2003) Methylene blue-treated fresh-frozen plasma: What is its contribution to blood safety? *Transfusion* 43(9):1322–1329.
24. Ergaieg K, Seux R (2009) A comparative study of the photoinactivation of bacteria by meso-substituted cationic porphyrin, rose Bengal and methylene blue. *Desalination* 246(1-3):353–362.
25. Wainwright M, Phoenix DA, Laycock SL, Wareing DRA, Wright PA (1998) Photobactericidal activity of phenothiazinium dyes against methicillin-resistant strains of Staphylococcus aureus. *FEMS Microbiol Lett* 160(2):177–181.
26. Wagner SJ, Skripchenko A, Robinette D, Foley JW, Cincotta L (1998) Factors affecting virus photoinactivation by a series of phenothiazine dyes. *Photochem Photobiol* 67(3):343–349.
27. Wainwright M, Mohr H, Walker WH (2007) Phenothiazinium derivatives for pathogen inactivation in blood products. *J Photochem Photobiol B* 86(1):45–58.
28. Chen J, Cesario TC, Rentzepis PM (2010) Time resolved spectroscopic studies of methylene blue and phenothiazine derivatives used for bacteria inactivation. *Chem Phys Lett* 498(1-3):81–85.
29. Usui Y (1965) Photoreduction of methylene blue and thionine in ethanol. *Bull Chem Soc Jpn* 38(2):206–215.
30. Danziger RM, Bar-Eli KH, Weiss K (1967) The laser photolysis of methylene blue. *J Phys Chem* 71(8):2633–2640.
31. Wotherspoon N, Oster G (1957) Light induced spectral shift of the thiazine dyes in the bound state. *J Am Chem Soc* 79(15):3992–3995.
32. Lindig BA, Rodgers MAJ, Schaap AP (1980) Determination of the lifetime of singlet oxygen in water-d2 using 9,10-anthracenedipropionic acid, a water-soluble probe. *J Am Chem Soc* 102(17):5590–5593.
33. Hatz S, Poulsen L, Ogilby PR (2008) Time-resolved singlet oxygen phosphorescence measurements from photosensitized experiments in single cells: Effects of oxygen diffusion and oxygen concentration. *Photochem Photobiol* 84(5):1284–1290.
34. Moan J, Berg K (1991) The photodegradation of porphyrins in cells can be used to estimate the lifetime of singlet oxygen. *Photochem Photobiol* 53(4):549–553.
35. Hoebeke M, Damoiseau X (2002) Determination of the singlet oxygen quantum yield of bacteriochlorin a: A comparative study in phosphate buffer and aqueous dispersion of dimiristoyl-L-alpha-phosphatidylcholine liposomes. *Photochem Photobiol Sci* 1(4):283–287.
36. Gandin E, Lion Y, Van de Vorst A (1983) Quantum yield of singlet oxygen production by xanthene derivatives. *Photochem Photobiol* 37(3):271–278.